JOURNAL OF MATERIALS SCIENCE 35 (2000) 5921 – 5925

Electrochemical behaviour of a type 302 stainless steel in a stress field

F. NAVAI*
Laboratoire de Génie des Matériaux, ISITEM, Université de Nantes, France

The 302 stainless steel type samples, were subjected to a U-bend test and the electrochemical behaviour of both the compressive and tensile strained surfaces of the samples were studied in a normal sulphuric acid bath. For this, the polarization curves $I = f(E)$, and current-time curves $I = f(t)$, were plotted separately for the concave and convex sides of each specimen. It was found that, the critical current density Icc, and passive current density Ip, are slightly less for the sides under compression than for the sides under tensile stress. Afterwards, some samples were subjected to a buckling test and the variation of electrode potential of each one of both sides of the samples stressed by buckling was studied separately. The obtained results show that the application of a tensile stress always leads to a decreasing potential of the convex side of samples; whereas a compression stress leads the potential of concave sides to more noble values. Therefore, it was shown that an assembly of two identical electrodes, electrically isolated, bent and immersed in the solution forms a "differential stress cell" with an electromotive force about thirty mV in equilibrium.

1. Introduction

Two metallic conductors, in contact with an electrolyte can form a galvanic cell producing a corrosive attack; and in several cases the Nernst equation allows to calculate the electromotive force of the cell. Some of the most common conditions which create galvanic cells are: two different metals coupled in the same electrolyte solution; two similar metals in different electrolyte solutions etc. . . [1].

Two similar metals (with the same chemical composition) coupled and immersed in a solution, can likewise form a galvanic cell provided that their areas have different physical conditions [1–3]. For example, when a metallic sample immersed to an electrolyte is subjected to tensile stress, its electrode potential becomes always anodic with respect to an unstressed sample [4, 5]. Contrary to the effect of tensile stresses on the electrochemical behaviour of alloys, the role played by the compressive stresses, in particular its effect on the variation of the electrode potential of specimens loaded under compressive stresses, is not well known.

It is evident that some behaviour of an alloy under compressive stress may be identical to those under tensile stress. For example the plastic deformation by compressive stress has the same effect on the passive film breaking than has tensile stress: in both cases the emergent slip step produced active fresh metal areas [6]. But, it can be also thought that because compressive stresses tend to close the cracks and reduce the real surface contact of the alloy with its environment, they should have a beneficial effect on the stress corrosion resistance of metallic alloys [7].

In fact, in a previous investigation [8], conducted by Auger electron spectroscopy, the influence of the tensile and compressive stresses on the composition and thickness of the passive films formed on the both sides of a bent sample in a normal sulphuric acid solution, was studied and it was found that the oxidation was greater on the convex side (under tensile stress) than on the concave side (under compressive stress) (Fig. 1).

In other words, the tensile stress increases the surface activity more than the compressive stress does, although, both sides of specimen just after electropolishing could be considered similar. This difference between the passivation behaviours of the opposite sides of the same specimen is due to the effect of stresses.

Consequently, the present investigation deals with the effects induced by the signs of stresses on the electrochemical parameters of electrodes.

2. Experimental procedure

2.1. Base material

In the present study two series of specimens are prepared: the dimensions of first one allotted to bending test are: 80 mm long, 8 mm wide and 0.25 mm thick, and those of the second one allotted to buckling test are $110 \times 8 \times 0.25$ mm. They were cut from a type 302 stainless steel sheet from Goodfellow, the composition of the steel investigated is indicated in Table I. The

*Author to whom all correspondence should be addressed.

TABLE I Chemical composition of the steel (wt%)

Cr	Ni	Mn	C	S	P	Fe
17–20%	7–11%	<2%	<0.16%	<0,03	<0,045	Balance

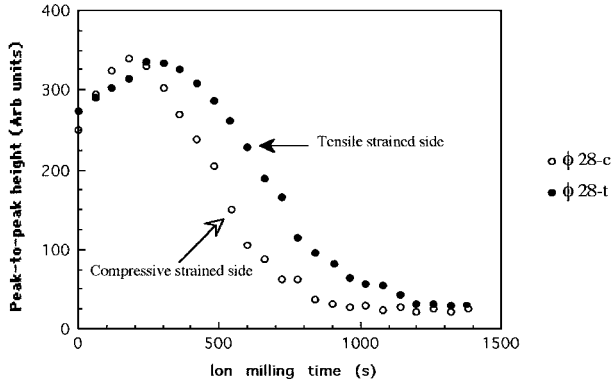

Figure 1 AES depth profiles for oxygen showing the effect of straining on the passive film width formed on both sides of a U-bend sample; radius of curvature ≈14 mm.

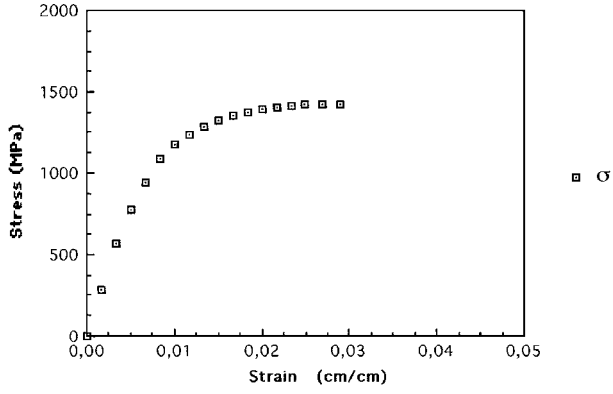

Figure 2 Stress-strain curve plotted for type 302 stainless-steel "Hard"; strain rate, $\varepsilon^{\circ} = 0{,}01666\ \text{min}^{-1}$.

longitudinal axes of the samples were oriented parallel to the prior rolling direction of the sheet. The principal mechanical properties of the type 302 "Hard" stainless steel are: Young's elastic modulus: 190 GPa, Hardness: 190 Brinell, and Ultimate Stress: 1450 MPa (Fig. 2).

2.2. Surface treatment

The test specimens received the following initial preparation. They were washed with soap, rinsed with water, ultrasonically degreased in an acetone bath. They were then electropolished in an 15% sulphuric acid ($d = 1.83$) and 85% orthophosphoric acid ($d = 1.70$) mixture, washed in doubly distilled water and finally dried with hot air. Then, prior to experiments, excepted the central portion of one of the two sides of each specimen (2 cm long and 8 mm width) was coated with epoxy resin.

2.3. Mechanical stressing

The Mechanical stressing for the samples allotted to buckling tests was carried out by tensile-machine. The others samples were bent into a U-shape using a mechanical system. Then, they were bowed at a radius of curvature $\rho = 14 \pm 1$ mm. The superficial layers strain ε, can be calculated from the following relationship:

$$\varepsilon = \frac{e}{2\rho} = \frac{0{,}11}{\rho} \qquad (1)$$

where e (≈0,22 mm) is the thickness of specimen after electropolishing and ρ is its radius of curvature.

2.4. Activation of specimens

Before the experiments, the area of the specimen to be exposed to the electrolyte solution was cleaned and rapidly electropolished again, then washed with doubly-distilled water. Afterwards, the specimen was immediately immersed in a desaerated 1 N H_2SO_4 solution.

In order to reduce the undesirable thin oxide layers formed on each sample surface before its introduction into the bath, the sample were cathodically pretreated: Firstly a negative linear scan was applied to electrode from 0 mV/SCE till the current density reached a value of $-0{,}200$ mA/cm^2, arbitrarily chosen for all samples. This value corresponds to a cathodic potential of about -550 mV/SCE, and then the cathodization was stopped.

3. Preliminary experiments

3.1. Polarization curves $I = f(E)$

Preliminary experiments were made to examine the influence of compressive and tensile stresses on the polarization curves $I = f(E)$. A platinum counter-electrode was used, and all potentials were measured with reference to a saturated calomel electrode (SCE). Potentiodynamic polarization experiments were carried out using a Taccussel automatic potentiostat.

After the cathodization proceeding, a positive linear scan is applied to the electrode with a scanning rate of 100 mV/min. The curves were plotted separately for the concave and convex sides of the U-bend samples ($\rho = 14 \pm 1$ mm.). Fig. 3 shows that, in a reproducible way, the critical current Icc, and anodic passive current Ip, are less for the side under compression than for

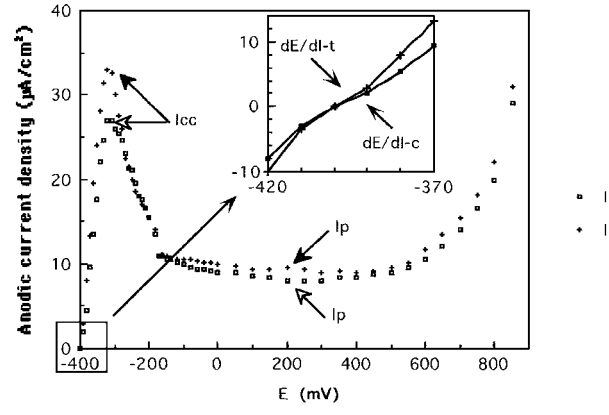

Figure 3 Polarization curve for both under compressive and tensile stresses sides of the U-bend samples in 1 N H_2SO_4 solution. Sample potential were measured against the saturated calomel electrode (SCE).

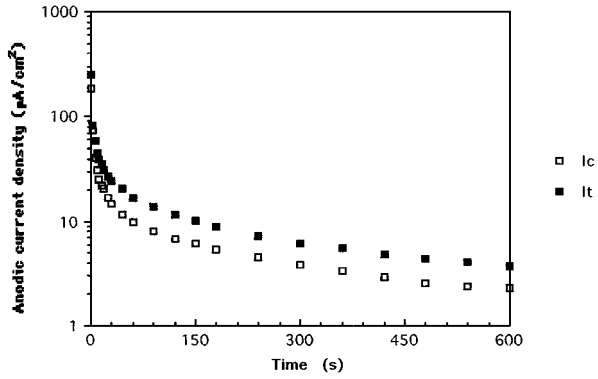

Figure 4 Influence of compressive and tensile stresses on the current-time curves of 302 samples at passive potential of +450 mV/ECS.

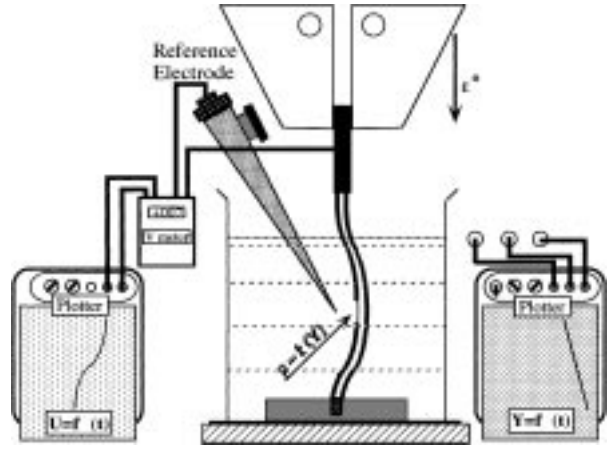

Figure 5 Testing unit allowing the measurement of potential versus stress.

the side under traction, proving that the passive film formed on the concave side is more protective than the one formed on the convex side.

In addition, the polarization resistance, the shape of the $E = f(I)$ curve at point $I = 0$, $\mathrm{d}E/\mathrm{d}I_I = 0$, for the convex side is slightly less in comparision with concave side: $R_c \approx 2{,}7$ kΩ/cm^{-2} and $R_t \approx 2{,}1$ kΩ/cm^{-2}. These values indicate that the passivation for the concave side occurs more rapidly than for the convex side.

3.2. Current-time curves $I = f(t)$

The variation of anodic current density versus time was studied separately for the convex and concave sides of the samples ($\rho = 14 \pm 1$ mm.). The passivation potential was +450 mV/SCE.

Effect of time on passive current density for both the compressive and tensile strained surfaces is shown in Fig. 4. It can be noticed that the anodic current density which is proportional to the dissolution rate of electrode [9], is higher for the tensile stressed side than for the compressive stressed one.

4. Results and discussion

4.1. Study of the potential of the electrode stressed by buckling

In this part of the work, the variation of the electrode potential of the non coated zone of each sample bent by buckling was studied versus the stress. All the more as the electrode potential is less sensitive to the surface roughness than the anodic current density is.

For the buckling experiment, the specimen prepared as described in 2.4. is placed in the vertical position and passes concentrically through the unit cell, being gripped at the upper end by the jaw of a conventional vertical tensile-testing machine (Adamel Lhomargy model DY25). The lower end was fixed at the bottom of the cell (Fig. 5). Then the sulphuric acid solution was poured into the cell.

It was necessary to wait for 60 to 120 minutes, to allow the electrode potential to reach an almost stationary value ($\approx$+5 mV/SCE). During this time the specimen became covered with a stable passivation film. Then, the motor of the tensile machine -working in compression- was switched on with a rate of 3 mm/min. In order to produce bending and imposing its concavity or convexity a lateral force is briefly applied and then the variation of electrode potential of the non coated zone of specimens was recorded. The electrode potential measurements were made with a high impedance voltmeter in series with a PL4 J. J. Lloyd recorder, and all potentials were measured with reference to a saturated calomel electrode (SCE).

The variation of the curvature radius of the specimen versus Y, $\rho = f(Y)$, was determined experimentally and shown in Fig. 6. This curve allows to plot the curve of the variation of electrode potential as a function of the curvature radius $U = f(\rho)$, (Fig. 7).

Considering the relationship (1) and having plotted the stress-strain curve $\sigma = f(\varepsilon)$ for this alloy (Fig. 2), the variation of stress in the outer layers versus the radius of curvature, $\sigma = f(\rho)$, can be determined, allowing finally to plot the curve of the variation of electrode potential for each side of the specimen, as a function of the passive film stress $U = f(\sigma)$, (Fig. 7). This figure shows that when stressing was started, even within the region of elastic deformation, the electrode potential of the convex side decreases with increasing stress, whereas, that of concave side becomes more noble.

In the plastic region, the decrease in potential of the convex side can be attributed to the emergent slip step surface producing fresh metal areas. But this model cannot explain the increase in potential of the concave

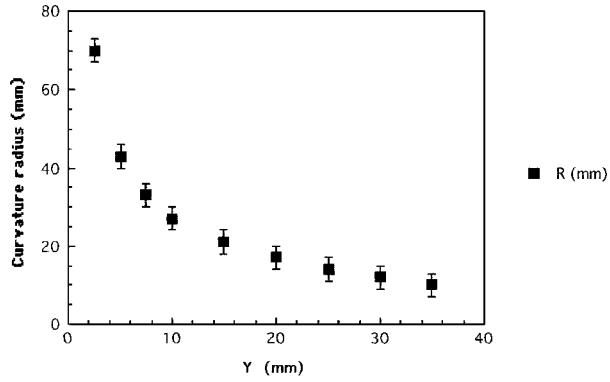

Figure 6 Variation of curvature radius ρ, versus the displacement of the jaw, Y.

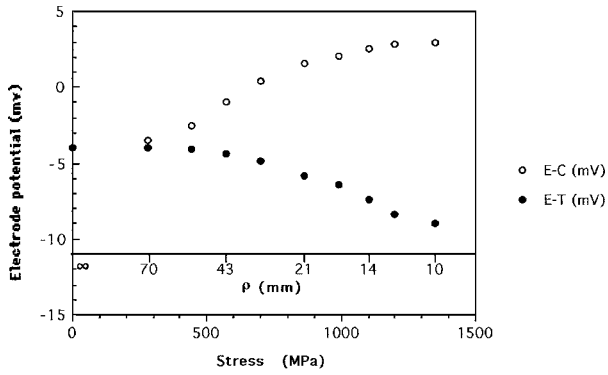

Figure 7 Variation of electrode potential of both the concave (E-C) and convex (E-T) sides of samples versus: a) radius of curvature ρ; b) stress in passive films σ.

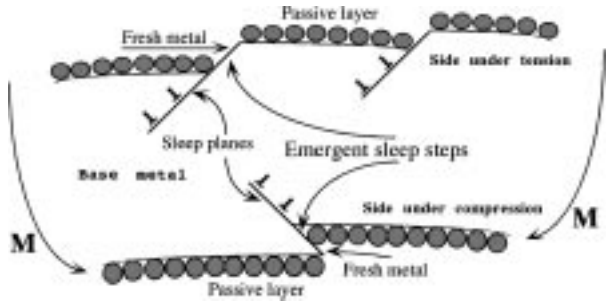

Figure 8 Schematic illustration of breaking of passive films on both sides under compression and tensile stresses of a U-bend specimen.

side. If the sample is plastically strained, the films on both sides of U-bend specimen are broken by emergent slip steps. Nevertheless, in this region, the reformation of film on the concave side can occur more rapidly because of its less large fresh surface area in contact with the environment [10] (Fig. 8).

In addition, concerning the elastic region, on the compressive stressed side, more compact, the passivation species, OH^-, O^{--} etc... [3], will rather have a tendency to remain as chemisorbed species; whereas, on the side under tensile stress, this tendency should be reduced, and the passive film, less impermeable, can facilitate the formation of non-stiochiometric metal oxide in the underlying metal layers.

On the other hand, the ductility of the passive film is an important parameter able to influence the surface potential of a strained sample within its elastic limit [11, 12]. Indeed, the width of a ductile passive film increases with increasing compressive stress, provided that the passive film total volume remains constant. Consequently, the electrode potential of the concave side tends toward noble values, because a high electric field strength exists within the passive film ($E \geq 10^8$ V/m) [13].

In addition, the elastic deformation leads to a change in the volume per atom [14] or to the dimensionless atom radius, r_s/a_0 is given by:

$$\frac{r_s}{a_0} = \left(\frac{3V}{4\pi N a_0^3}\right)^{1/3} \tag{2}$$

Where N is the number of free electrons in the volume V and r_s is the radius of a sphere whose volume is equal to the volume per conduction electron and a_0 is the Bohr radius ($\approx$0,529 Å). then the strain ε, can be written:

$$\varepsilon = \frac{\Delta r_s}{r_s} \tag{3}$$

Thus, a tensile stress increase the volume per atom ($\varepsilon > 0$) whereas a compressive stress decrease it ($\varepsilon < 0$).

Because of this variation of local volume per atom, a redistribution of the free electrons in the metal must occur in order to equalize their electrochemical potential [15]. This redistribution of free electrons creates a macro-potential change in the metal ΔU, whose sign depends on the sign of stress. In fact, the region under compressive stress, with a reduced local volume per atom, will have a macropotential change with an opposite sign in comparison with the region under tensile stress where the local volume per atom is enhanced [15]. Consequently, between two electrodes (or between two region of the same metal) under stresses of different signs, it must appear a potential difference due to this redistribution. In the same way, the variation of the dimensionless atom radius modifies the work function of free electrons and the barrier potential of electrodes.

Tiller and Schrieffer [16], used the approximations suggested by Wigner [17] and by Gell-Mann and Breuchner [18], and evaluated this macropotential $\Delta\Phi$, for the dimensionless atom radius r_s/a_0 ranging from 2 to 3: $\Delta\Phi = -80$ mV/ ε%. This potential is relative to ahead of crack tip, they expect this potential to fall up sharply in the non-linear elastic region to a value of about -10 to -20 mV/ ε% in 10–20 atom distances. These values were approximately, in agreement with the results obtained in this investigation [19].

4.2. Formation of a differential stress cell

The results obtained above lead to prediction of the formation of a differential stress cell, between the areas of two similar metals where one is under compression and the other under tension.

Therefore, an assembly of two electrodes, isolated with a flexible resin (except the external central portion of each one) was prepared and deformed at U-form. This assembly was then immersed in a desaerated normal sulphuric acid solution (Fig. 9). After cathodic activation, the potential difference between these electrodes against time was recorded.

The electrode whose convex side was in contact with electrolyte was connected to the negative input of recorder.

Fig. 10 shows the potential difference between the electrodes ΔU, versus time. Analysis of this curve shows that during 20–30 minutes, just after cathodic activation, ΔU is not stabilized: the potential of the concave side at first becomes (during 0,5–1 minute) more noble with respect to the convex side ($\Delta U > 0$) then it shifts rapidly to more negative values, and the curve passes through a minimum, ($t \approx 1$ min;

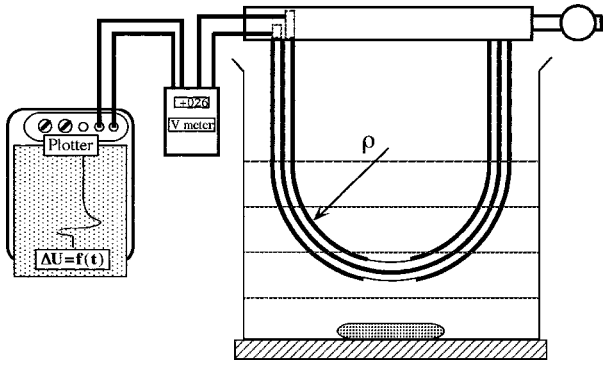

Figure 9 Testing unit allowing to study the potential difference variation between the tensile and compressive stressed sides of two specimens deformed to U-form.

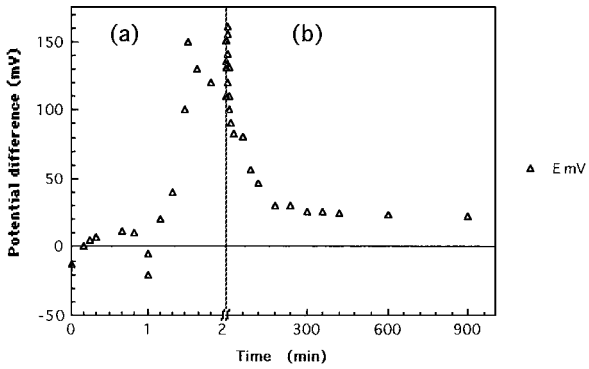

Figure 10 Potential difference between the tensile and compressive stresses sides of two isolated bent samples immersed in a H_2SO_4 solution against time, (a) for two first min; (b) continuation of the curve for $t > 2$ min.

$\Delta U \approx -25$ mV). Then, ΔU becomes more noble again at the same rate, then passes through a maximum ($\Delta U \approx 150$ mV), and finally decreases and becomes later approximately stable at $\Delta U \approx 26$ mV. The potential difference between both electrodes decrease, can be attributed to the passivation and the change in thickness of the passive films formed on the surfaces in contact with solution [5].

In equilibrium, the electrode potential of the concave side is cathodic with respect to the convex side forming a differential stress cell. The electromotive force of the differential stress cell, in addition of usual factors as temperature, pH of solution etc. . ., depends principally upon the following parameters: The nature and mechanical behaviour of the electrode, especially its yielding point and its ultimate tensile stress; the strain or radius of curvature of the electrodes; the composition and aggressivity of the solution; and the logarithmic creep (primary creep) generating the active fresh metal areas.

5. Conclusions

The electrochemical behaviour of type 302 stainless steel samples deformed at U-form was investigated. The effects of tensile and compressive stresses upon the polarization curves, and upon the current-time diagram of samples passivated under the applied potential of +450 mV/SCE in a normal sulphuric acid solution at room temperature were examined.

The variation of the electrode potential versus time for both the concave and convex sides of specimens stressed by buckling was also studied, and the formation of a differential stress cell was carried out.

On the basis of the results obtained in this work, the following conclusions may be drawn:

1. The critical current Icc and anodic passive current Ip are slightly enhanced under tensile straining effect and reduced under compressive straining; i.e. the passive film formed on the concave side is more protective than it is on the convex side.

2. The polarization resistance is less for tensile stressed side than for the compressive stressed one; i.e. the passivation for the concave side occurs more rapidly than for the convex side.

3. The electrode potential of the convex side of the sample becomes less noble with increasing tensile stress. On the contrary, an increase of the compressive stress leads to an increase in the nobility of the potential.

4. Two similar electrodes where one is subjected to a tensile stress and the other to compressive stress (or the opposite sides of a U-bend specimen), coupled and immersed in the same electrolyte, form a differential stress cell with the compressive strained surface acting as a cathode.

References

1. T. HOWARD ROGERS, "Marine Corrosion," General Editor L. L. Shreir (London, 1967) p. 25.
2. H. H. UHLIG, "Corrosion and Corrosion Control" (John Wiley & sons, Inc. (ed.), New York, 1963) p. 10.
3. H. H. UHLIG, *Corrosion Science* **9** (1979) 777.
4. A. V. RYABCHENKOV and V. M. NIKIFAROVA, in "Intercrystalline Corrosion and Corrosion of Metals under Stress," edited by I. A. Levin (New York, 1962) p. 161.
5. T. P. HOAR and J. G. HINES, *Journal of the Iron and Steel Institute* **182** (1956) 124.
6. H. L. LOGAN, *Journal of Research of the National Bureau of Standards* **48** (1952) 99.
7. T. MAGNIN and L. COUDREUSE, *Acta Metall.* **53** (1987) 2105.
8. F. NAVAÏ, *Journal of Materials Science* **30** (1995) 1166.
9. T. P. HOAR and J. R. GALVELE, *Corrosion Science* **10** (1970) 211.
10. R. W. STAEHLE, in "Stress Corrosion Cracking and Hydrogen Embattlement of Iron Base Alloys, Vol-5" (NACE, 1977) p. 180.
11. F. NAVAÏ, *Matériaux & Techniques* **12** (1995) 30.
12. S. F. BUBAR and D. A. VERMILYEA, *J. Electrochem. Soc.* **113** (1966) 892.
13. J. C. SCULLY, in Atomistics of fracture, NATO Conference, 1983, edited by R. M. Latanision and J. R. Pickens, p. 652.
14. N. W. ASHCROFT and N. D. MERMIN, "Solid State Physics," International ed. (USA, 1990) p. 4.
15. W. A. TILLER, in "Stress Corrosion Cracking and Hydrogen Embrittlement of Iron Base Alloys, Vol. 5," edited by Unieux-Firminy (NACE, Houston, Texas, 1973) p. 332.
16. W. A. TILLER and R. SCHRIEFER, *Scripta Metallurgica* **4** (1970) 57.
17. E. WIGNER and F. SEITZ, *Physical Review* **43** (1933) 804.
18. M. GELL-MANN and K. BRUECKNER, *Physical Review* **106** (1957) 364.
19. F. NAVAÏ, Thesis, ISITEM, Université de Nantes, 1997.

Received 27 August 1999
and accepted 3 February 2000